Carbohydrate Polymers 90 (2012) 583–591

Contents lists available at SciVerse ScienceDirect

Carbohydrate Polymers

journal homepage: www.elsevier.com/locate/carbpol

Polylactide-based renewable composites from natural products residues by encapsulated film bag: Characterization and biodegradability

Chin-San Wu*

Department of Chemical and Biochemical Engineering, Kao Yuan University, Kaohsiung County 82101, Taiwan, ROC

ARTICLE INFO

Article history:
Received 7 July 2011
Received in revised form 3 April 2012
Accepted 22 May 2012
Available online 9 June 2012

Keywords:
Polylactide
Recycled corn starch
Biodegradation
Controlled release
Fertilizer utilization promoted bacterial

ABSTRACT

In the present study, the biodegradability, morphology, and mechanical properties of composite materials consisting of acrylic acid-grafted polylactide (PLA-g-AA) and natural products residues (corn starch, CS) were evaluated. Composites containing acrylic acid-grafted PLA (PLA-g-AA/CS) exhibited noticeably superior mechanical properties due to their greater compatibility with CS compared with PLA/CS. The feasibility of using PLA-g-AA/CS as a film bag material to facilitate the controlled release of an encapsulated phosphate-solubilizing bacterium (PSB) *Burkholderia cepacia* as a fertilizer use promoter was then evaluated. For purposes of comparison and accurate characterization, a PLA film bag was also assessed. The results showed that the bacterium completely degraded both the PLA and the PLA-g-AA/CS composite film bags, resulting in cell release. The PLA-g-AA/CS (20 wt%) film bags were more biodegradable than those made of PLA, and displayed a higher loss of molecular weight and intrinsic viscosity, indicating a strong connection between these characteristics and biodegradability.

1. Introduction

Although recycling is an environmentally attractive solution, the disposal of non-biodegradable plastics has caused extensive environmental problems. Moreover, only a small percentage of plastics are recyclable, the majority ending up in municipal landfills, which have limited availability. As a result, there is increased interest in the production and use of biodegradable polymers from renewable and/or fossil sources, for economical and environmental reasons, such as waste management and carbon emissions (Arvanitoyannis, Ladas, & Mavromatis, 2006; Lu, Lu, He, & Yu, 2009). The use of biodegradable polymers in the packaging industry and in the agricultural sector and other disposable articles places special requirements on this material. Ideally, such materials should be part of the natural life cycle of biomass (i.e., the raw materials should be renewable and biodegradable to harmless, natural products (Kayserilioglu, Bakir, Yilmaz, & Akkas, 2006; Nyambo, Mohanty, & Misra, 2010; Torbica, HadnaCev, & Dapcevi, 2010).Polylactide (PLA) belongs to the family of synthetic aliphatic polyesters and is considered to be biodegradable; it decomposes rapidly in a typical compost environment (Cornelissen et al., 2008; Wang & Lis, 2008). PLA can degrade into components with less than 10 lactic acid and monomer units, and has been reported to possess plant growth-stimulatory activity (Tuominen et al., 2002). Furthermore, PLA is a thermoplastic, high-strength, high-modulus polymer that can be made from renewable resources, including corn, sugar beets, and rice (Gupta, Revagade, & Hilborn, 2007). In contrast to conventional plastics, such as polypropylene (PP) and polyethylene (PE) that require hundreds or even thousands of years to degrade, PLA can degrade into naturally occurring products in just a few years (Wang et al., 2008). However, PLA production is both complex and expensive, limiting its commercial applications. This limitation can be overcome by blending PLA with cost-effective biodegradable natural biopolymers, such as natural products residues (corn starch, wheat straw, rice flour), which are often used as they are abundant, inexpensive, renewable, and fully biodegradable materials (Dias, Müller, Larotonda, & Laurindo, 2010; Gupta & Kumar, 2007; Liu, Jiang, Liu, & Zhang, 2010; Nair & Laurencin, 2007; Shah, Hasan, Hameed, & Ahmed, 2008). While blending PLA and natural products residues markedly reduces cost and enables flexibility in adjusting the biodegradability and mechanical properties of the hybrid products, the natural products residues are fairly hydrophilic, meaning poor compatibility between the two phases occurs. To address this problem, reactive functional groups may be incorporated into the polymer as compatibilizers, to enhance the miscibility of the two polymers and improve the overall mechanical properties of the blend (Yu, Dean, & Li, 2006). Maleated polylactide copolymers have been shown to be effective compatibilizers in polylactide/natural fiber composites, and coupling agents have been used to reinforce polylactide/recycled wood fiber composites (Pilla, Gong, Neill, Yang, & Rowell, 2009; Wu, 2009). Composites of PLA and natural products residues thus offer advantages in both biocompatibility and cost (Jacobsen, Fritz, Degee, Dubois, & Jerome, 2000; Nampoothiri, Nair, & John, 2010) and display complete

* Tel.: +886 7 6077685; fax: +886 7 6077788.
E-mail address: t50008@cc.kyu.edu.tw

0144-8617/$ – see front matter © 2012 Elsevier Ltd. All rights reserved.
http://dx.doi.org/10.1016/j.carbpol.2012.05.081

degradation in soil or compost without the emission of toxic or noxious components.

The aim of this study was to investigate PLA as a core matrix, blending it with natural products residues to modify its physical properties, including biodegradability and permeability. To overcome the problem of poor adhesion of corn starch-polymer composites, an AA-grafted composite was selected as a compatibilizer, and PLA-g-AA/CS was compared with PLA. PLA-g-AA/CS and PLA were used to encapsulate cells of an indigenous phosphate-solubilizing bacteria (PSB) strain (*Burkholderia cepacia*), and changes in the structure and biodegradability of the bacteria-encapsulated film bag (BEFB) in saline, fertilizer solution, and cultivated land were examined. The main objective was to assess the feasibility of the use of the PLA/corn starch-type composite as a material for a controlled-release film bag system for application in bacteria-promoted fertilizer.

Phosphorus, deficiency of which restricts plant growth in soil, is one of the essential macronutrients required for the growth of plants, but excessive addition of chemically synthesized fertilizers for crop production has led to the deterioration of farmland quality because of insoluble phosphate complexes in the soil (Kidd, Domínguez-Rodríguez, Díez, & Monterroso, 2007). This problem has motivated the use of more environmentally friendly fertilizers for sustainable land use. PSBs are bacteria-promoted fertilizers that are one of the most popular choices for bacteria-encapsulated film bags (Kumar, Bajpai, Dubey, Maheshwari, & Kang, 2010; Liu, Wu, & Chang, 2008). PSBs can mobilize and solubilize insoluble phosphate compounds accumulated in soil through chelation, biotic acidification, and exchange reactions, thereby allowing crops to use the soluble phosphate compounds released from the soil without the need for additional phosphate fertilizers (Hamdali, Hafidi, Virolle Marie, & Ouhdouch, 2008; Junli et al., 2009; Mamta et al., 2010; Son, Park, Cha, & Heo, 2006). However, an effective method to inoculate bacteria into the soil and maintain their viability and function during crop cultivation is still required. Encapsulating the bacteria in biodegradable film bags, which protect the cells while allowing their controlled release into the soil, is beneficial. The effectiveness and stability of BEFB can be markedly enhanced. A key issue in the development of controlled-release of BEFB is designing and developing suitable biodegradable materials for these controlled-release film bags.

2. Experimental

2.1. Materials

Polylactide, composed of 95% L-lactide and 5% meso-lactide and with a molecular weight (M_w) of 9.86×10^4, a molecular weight number (M_n) of 5.21×10^4, a polydisperity index of 1.89, was used as supplied by Nature Works Corporation (Nebraska, USA). Acrylic acid (AA) was obtained from Sigma (St. Louis, MO, USA), and purified prior to use by recrystallization from chloroform. Benzoyl peroxide (BPO; Sigma) was used as an initiator and was purified by dissolution in chloroform and re-precipitation in methanol. A corn residue composed of 27% amylose and 73% amylopectine was obtained from the Corn Refiners Association, Inc. (Washington, USA). The levels of protein and lipid in the corn residue were insignificant. To acquire the natural product, crude corn residue was firstly air-dried at 105 °C for 1 day and vacuum-dried at the same temperature for another day until the moisture content decreased to 5 ± 2% (Scheme 1(A)). Dried corn residue was then crushed and passed through 80-mesh sieve to have corn starch powder with size at about 5–25 μm. PLA-g-AA was constructed in our laboratory according to procedures described in our previous work (Wu, 2005), and had a M_w of 9.26×10^4, a M_n of 4.52×10^4, a polydisperity index of 2.05. As the grafting percentage of PLA-g-AA was only about 6.02 wt%, the structure of PLA-g-AA was not noticeably different to that of PLA, and the physical properties varied only slightly. A slight decrease in molecular weight is apparent in PLA-g-AA, due to some cracking of the bond in the grafting.

2.2. Graft reaction and sample preparation

AA was grafted onto PLA dissolved in xylene under a nitrogen atmosphere at 80 ± 2 °C. The polymerization reaction was initiated with 0.3 wt% BPO, and the reaction system was stirred at 60 rpm for 8 h. The grafted product (4 g) was then dissolved in 200 mL refluxing xylene at 80 ± 2 °C, and the hot solution was filtered through several layers of cheesecloth. The cheesecloth was washed with 600 mL of acetone to remove xylene-insoluble unreacted AA, and the remaining product was dried in a vacuum oven at 80 ± 2 °C for 24 h. The xylene-soluble product in the filtrate was extracted five times using 600 mL of cold acetone each. Subsequently, the grafting percentage was determined using a titration method (Wu, 2005), revealing a grafting percentage of ~6.02 wt%. BPO and AA loadings were maintained at 0.3 and 10 wt%, respectively. The CS was fixed at a weight ratio of CS/PLA or CS/PLA-g-AA as 10/90, 20/80, 30/70, 40/60, and 50/50 by the melt blending method using a Plastograph 200 Nm mixer (W50EHT; Brabender GmbH, Duisburg, Germany) with a blade-type rotor. PLA or PLA-g-AA were placed into the Brabender instrument for melting at 50 rpm and 190 ± 5 °C. When the PLA or PLA-g-AA had melted completely, the dried CS was added into the mixer and blended for 15 min (Scheme 1(A)). The product was formed into 1-mm plates using a hot press, which were placed in a dryer for cooling. The thin plates were then made into the standard specimens for characterization.

2.3. Microorganism and culture medium

Burkholderia cepacia (BCRC 14256) was supplied by the Bioresource Collection and Research Center in Taiwan and cultivated at 37 °C at 200 rpm in nutrient broth (NB; Merck KGaA, Darmstadt, Germany). The broth consisted of 3 g beef extract, 5 g peptone, and 1.0 L of distilled water, pH 7.0. The culture was collected in the early stationary phase for cell entrapment.

2.4. Cell release experiments and fertilizer tests

Cell-loaded capsules were suspended in saline solution (0.85% NaCl), and the cell concentration monitored over time. Cell concentration was determined by counting the CFUs present on the NB agar plates after serial dilution and overnight incubation at 30 °C. For the controlled-release bacterial test, encapsulated 6.00 ± 0.05 × 6.00 ± 0.05 mm (0.05 ± 0.02 mm thickness) film bags were prepared from conditioned PLA, PLA/CS, or PLA-g-AA/CS matrix using the BEFB material, and a fixed volume (5 mL) of 1 mL *B. cepacia* containing 2.2 mg of cells (ca. 2.1×10^9 cells) and 4 mL fertilizer solution were injected into the BEFB (Scheme 1(B)). The cell-loaded film bags were immersed in sterile saline solution (0.85% NaCl) with an initial pH of 7.0 ± 0.2 and incubated at 37 °C. Under such conditions, Scheme 1(B) shows that *B. cepacia* was a rod-shaped bacterium of 0.8–2.6 μm × 0.5–1.1 μm and noticeable degradation of the PLA-g-AA/CS (20 wt%) matrix that encapsulated the *B. cepacia* cells for 20 days was evident, suggesting that the bacteria entrapped in the composites were alive and possessed normal functionality under the phosphate-solubilizing conditions. The extent of capsule degradation was monitored at designated 20 day time intervals. The cell concentration in the solution was determined by CFU counting on NB agar plates after serial dilution and overnight incubation at 30 °C, allowing the release of the cells to be assessed.

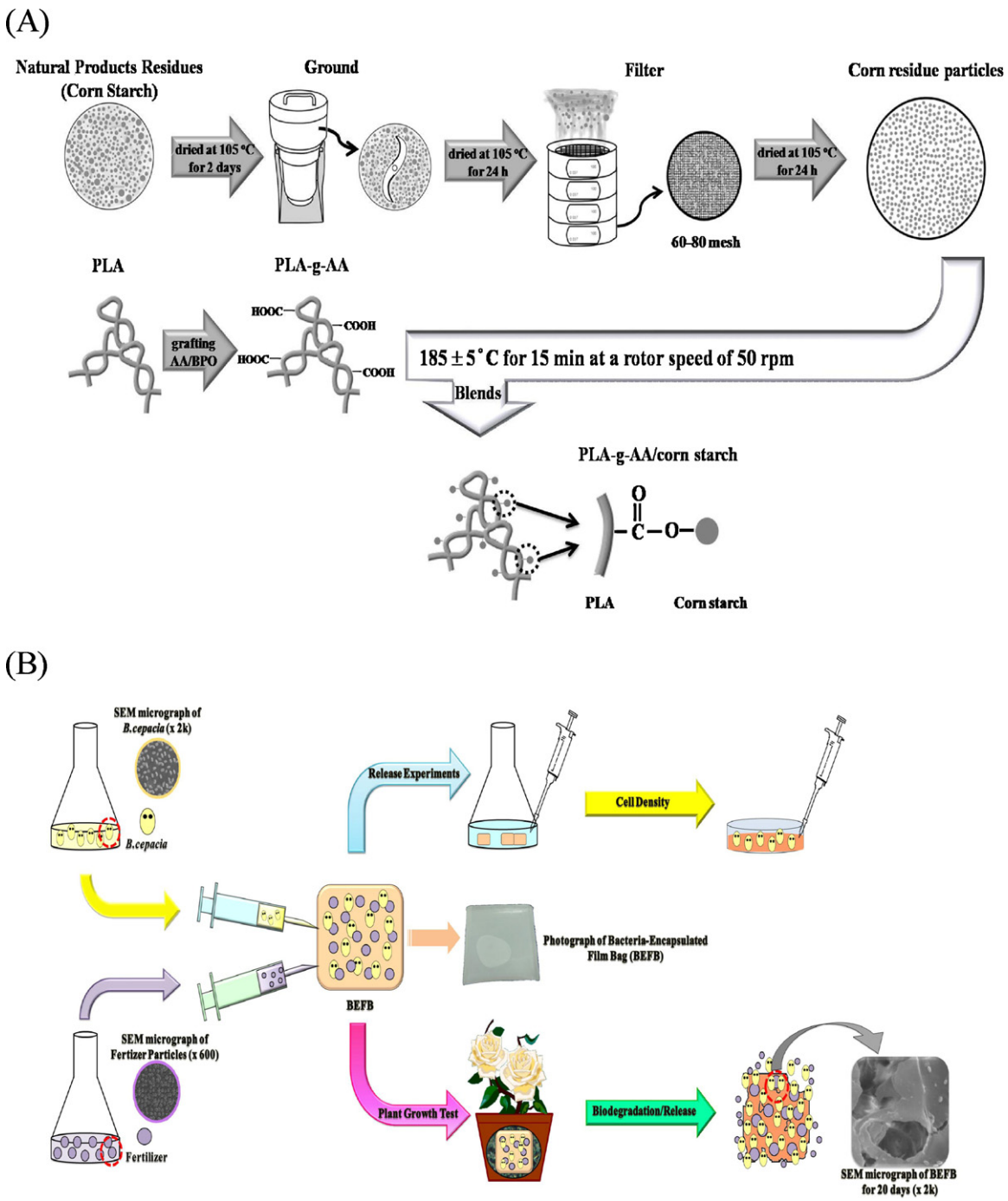

Scheme 1. (A) Modification of PLA, preprocess of natural products residues (corn starch), and the preparation of composite materials. (B) Images of the PLA-g-AA/CS (20 wt%) matrix BEFB samples loaded with a fixed volume (*B. cepacia* and fertilizer solution) and the preparation of biodegradation, cell release, and plant growth assays with BEFB.

To compare the effects of *B. cepacia* in the fertilizer, BEFB (Scheme 1(B)) was injected into 4 mL of fertilizer solution. The fertilizer was an inorganic compound fertilizer (N:P:K rate = 1:3:2; Taiwan Horticultural Co. Ltd., Taipei, Taiwan), 1 g of which was dissolved in 500 mL of water. Fig. 1A shows the surface morphology of the fertilizer particles (7–12 μm) without BEFB, and the size of the fertilizer particles without variation after 40 days (Fig. 1C). However, the fertilizer particles paste spread after 40 days, due to the addition of BEFB. According to these results, *B. cepacia* can spread the fertilizer particles, increasing their absorption by plants.

2.5. Characterization of PLA and composites

Solid-state ^{13}C nuclear magnetic resonance (NMR) was performed with an AMX-400 NMR spectrometer (Bruker, Billerica, MA, USA) at 100 MHz under cross-polarization while spinning at the magic angle. Power decoupling conditions were set with a 90° pulse and a 4 s cycle time. FTIR sample spectra were obtained using a FTS-7PC-type Fourier-transform infrared spectrophotometer (Bio-Rad, Hercules, CA, USA), while gel-permeation chromatography (GPC) was performed at 40 °C using a Perkin Elmer Series 200 system (Waltham, MA, USA) equipped with a Gel Divinylbenzene 10000As

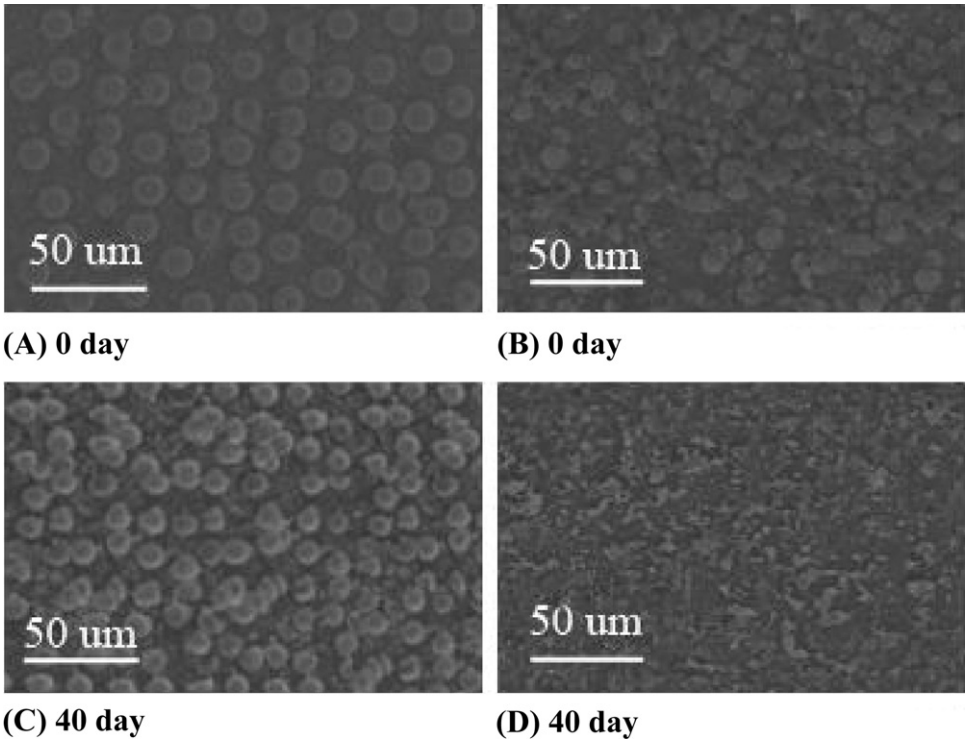

Fig. 1. SEM surface morphology of fertilizer particles without BEFB for (A) 0 days and (C) 40 days and fertilizer particles with BEFB for (B) 0 days and (D) 40 days (600× magnification).

(Jordi, Bellingham, MA, USA) instrument. The gel columns possessed a Refractive Index Detector RI-71 (Shodex, Tokyo, Japan) and polystyrene was used as a standard.

A capillary viscometer (Schott AG, Mainz, Germany) was used to measure the intrinsic viscosity of PLA or PLA-g-AA/CS dissolved in the chloroform solvent at various concentrations (0.5, 1.0, 1.5, and 0.2 g/dL). The solutions were cleared through a 0.45-μm filter (Lida, Kenosha, WI, USA) and the capillary viscometer was filled with 10 mL of sample and equilibrated in a water bath (B801; Schott AG) at 30.0 ± 0.1 °C. Each sample was passed through the capillary tube prior to flow time measurements. The flow time was used to calculate the relative and reduced viscosities, which were plotted against concentration, while the intercept demonstrated the intrinsic viscosity. An Instron mechanical tester (Model LLOYD, LR5K type) was used to measure the tensile break strength in accordance with the ASTM D638. Test samples were prepared in a hydrolytic press at 190 ± 5 °C and conditioned at 50 ± 5% relative humidity for 24 h prior to measurements. Measurements were performed using a crosshead speed of 20 mm/min. Five measurements were performed for each sample and the mean values were determined. After treating the samples with glutaraldehyde and immersion in 50–100% acetone solution, the samples were dried at 50 °C for 48 h and coated with gold. The morphologies were observed with a scanning electron microscope (SEM; model S-4100; Hitachi, Tokyo, Japan).

3. Results and discussion

3.1. Characterization of PLA and composite film bag materials

To identify structural differences between PLA and their composites, FTIR and NMR were used to characterize the BEFB materials. The FTIR spectra of unmodified PLA and PLA-g-AA are shown in Fig. 2A and B, respectively. The characteristic transitions of PLA at 3200–3800, 1700–1770, and 500–1500 cm^{-1} appeared in the spectra of both polymers, with an extra shoulder observed at 1710 cm^{-1} in the modified PLA spectrum. These features are characteristic of carboxyl groups. Similar results have been reported (Janorkar, Luo, & Hirt, 2004; Sullad, Manjeshwar, & Aminabhavi,

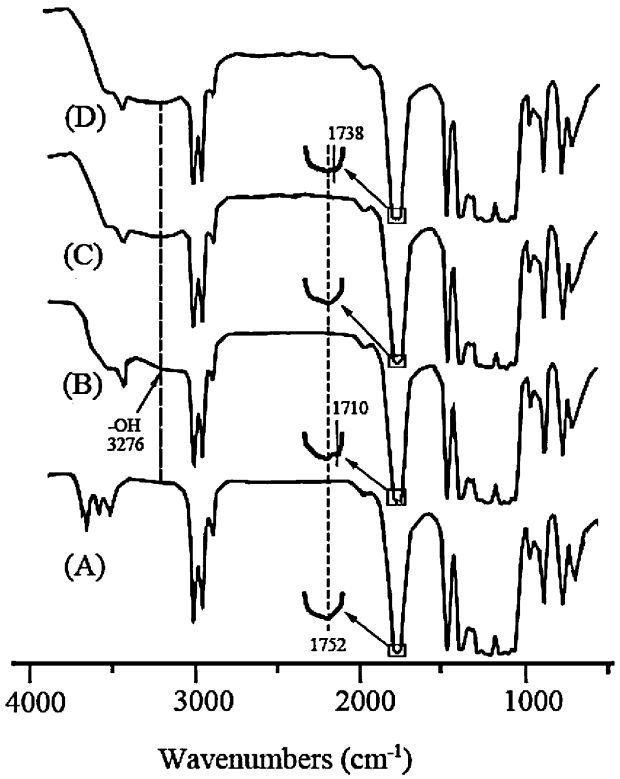

Fig. 2. Fourier-transform infrared spectroscopy spectra of (A) PLA, (B) PLA-g-AA, (C) PLA/CS (20 wt%), (D) PLA-g-AA/CS (20 wt%), and (E) CS.

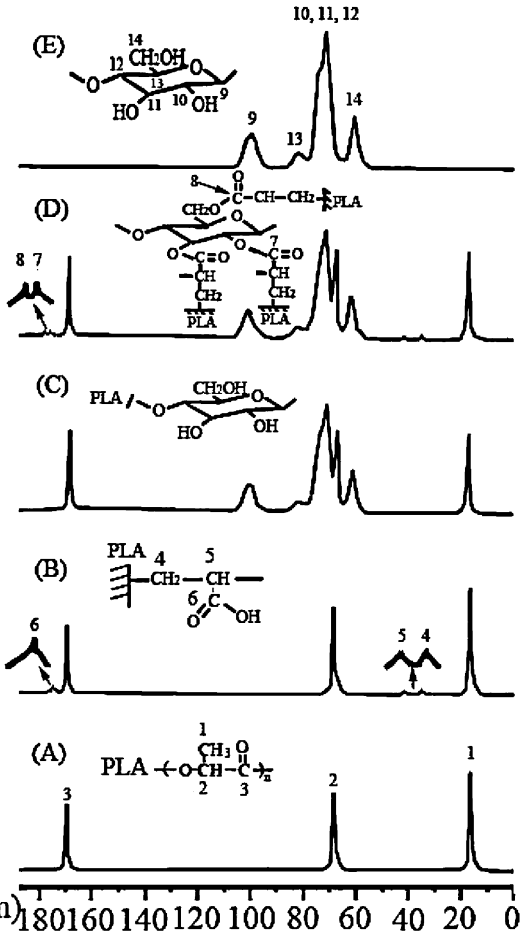

Fig. 3. Solid-state ^{13}C nuclear magnetic resonance spectra of (A) PLA, (B) PLA-g-AA, (C) PLA/CS (20 wt%), (D) PLA-g-AA/CS (20 wt%), and (E) CS.

2010). The shoulders represent free acid in the modified polymer and thus indicate the grafting of AA onto PLA.

The peak assigned to the O—H stretching vibration at 3200–3800 cm^{-1} intensified in the composite PLA/CS (20 wt%; Fig. 2C) due to the contribution of the —OH group of CS. The FTIR spectrum of the PLA-g-AA/CS (20 wt%) revealed a peak at 1738 cm^{-1} that was not present in the FTIR spectrum of the PLA/CS (20 wt%; Fig. 2D). This peak was assigned to the ester carbonyl stretching vibration of the copolymer. Gong, Wang, and Tu (2006) also reported an absorption peak at 1740 cm^{-1} for this ester carbonyl group. These data suggest the formation of branched and cross-linked macromolecules in the PLA-g-AA/CS composites by a covalent reaction of the carboxyl groups in PLA-g-AA with the hydroxyl groups of CS.

To further confirm this finding, solid-state ^{13}C NMR spectra of PLA and PLA-g-AA are compared in Fig. 3A and B, respectively. Three peaks were observed, corresponding to carbon atoms in the unmodified PLA ((1) δ = 16.92 ppm; (2) δ = 68.77 ppm; (3) δ = 169.92 ppm) (Zell et al., 1998). The ^{13}C NMR spectrum of PLA-g-AA showed additional peaks ((4) δ = 35.63 ppm; (5) δ = 42.23 ppm; (6) δ = 175.05 ppm), confirming that AA was grafted covalently onto PLA.

The solid-state ^{13}C NMR spectra of PLAA/CS (20 wt%), PLA-g-AA/CS (20 wt%), and CS are shown in Fig. 3C–E. Relative to unmodified PLA, additional peaks were observed in the spectra of composites containing PLA-g-AA. These additional peaks were located at δ = 35.63 ppm (4) and δ = 42.23 ppm (5). These same features were observed in previous studies (Wu, 2005) and

Table 1
The CS phase size of PLA/CS and PLA-g-AA/CS composites at different CS contents.

CS (wt%)	Phase size (μm)	
	PLA/CS	PLA-g-AA/CS
10	9.0 ± 1.0	5.0 ± 0.6
20	11.0 ± 2.0	6.0 ± 0.7
30	13.5 ± 2.5	6.5 ± 0.9
40	16.0 ± 3.0	6.9 ± 1.0
50	17.5 ± 3.5	7.3 ± 1.2

indicate grafting of AA onto PLA. However, the peak at δ = 175.05 ppm ((6) C═O; Fig. 3B), which is also typical for AA grafted onto PLA, was absent in the solid-state PLA-g-AA/CS (20 wt%) spectrum. This occurrence was most likely the result of an additional condensation reaction between the carboxyl group of AA and the —OH group of CS, causing a peak at δ = 175.05 ppm that was split into two bands (δ = 177.06 and 178.26 ppm). This additional reaction converted the fully acylated groups in the original CS to esters (represented by peaks 7 and 8 in Fig. 3D) and did not occur between PLA and CS, as indicated by the absence of the corresponding peaks in the FTIR spectrum of PLA/CS (20 wt%; Fig. 3C). The formation of ester groups significantly affects the thermal and biodegradation properties of PLA-g-AA/CS and is discussed in greater detail in the following sections.

3.2. Morphology and mechanical properties of PLA and composite film bag materials

It is necessary to study the morphology of the polymer composites as these dictate the mechanical properties. In the PLA/CS composites, PLA forms the matrix and CS the dispersed phase. SEM micrographs of PLA/CS (20 wt% and 40 wt%) and PLA-g-AA/CS (20 wt% and 40 wt%) composites are presented in Fig. 4A, while the CS phase size (the average pore diameter) of composites is tabulated in Table 1. By examining the morphology of the PLA/CS composites, it is evident that the size of the CS phase increased with increasing content of CS (Table 1). It is notable that in the PLA/CS composites containing less than 10 wt% CS, a fine dispersion and homogeneity of CS in the PLA matrix is present. The large size of CS phases, particularly in the composite containing 50 wt% CS, suggests that the adhesion between CS and PLA is poor and that the two polymers are strongly incompatible (Huang, Roan, Kuo, & Lu, 2005).

When the PLA-g-AA copolymer was added as the compatibilizer, the size of the CS phase reduced compared with the respective uncompatibilized composites. The ~11.0 ± 2.0 μm average pore diameter of PLA/CS (20 wt%; Fig. 4A) was larger than the ~6.0 ± 0.7 μm diameter of PLA-g-AA/CS (20 wt%; Fig. 4A). Moreover, Table 1 shows a fine dispersion and homogeneity of CS in the PLA-g-AA matrix for all compatibilized composites with a CS content of up to 50 wt%. The phase size in all compatibilized composites is lower than 9.0 ± 1.0 μm and is detectable only at the higher magnification. This increased dispersion arises from the formation of branched and crosslinked macromolecules caused by the reaction of carboxyl groups of the PLA-g-AA copolymer with the hydroxyl groups of CS. It is also pointed out bridging structure between CS and PLA-g-AA was formed during melt blending. This results in a reduction in the interfacial tension between the two polymers and a finer distribution of CS in all the compatibilized composites.

Fig. 4B shows the effects of the CS content on tensile strength at breakpoint for PLA/CS and PLA-g-AA/CS composites. For PLA/CS composites, tensile strength at breakpoint decreased continuously as the CS content increased. The composite containing 50 wt% CS gave the lowest tensile strength at breakpoint because the higher CS content increased with the phase size. It is thus clear that the

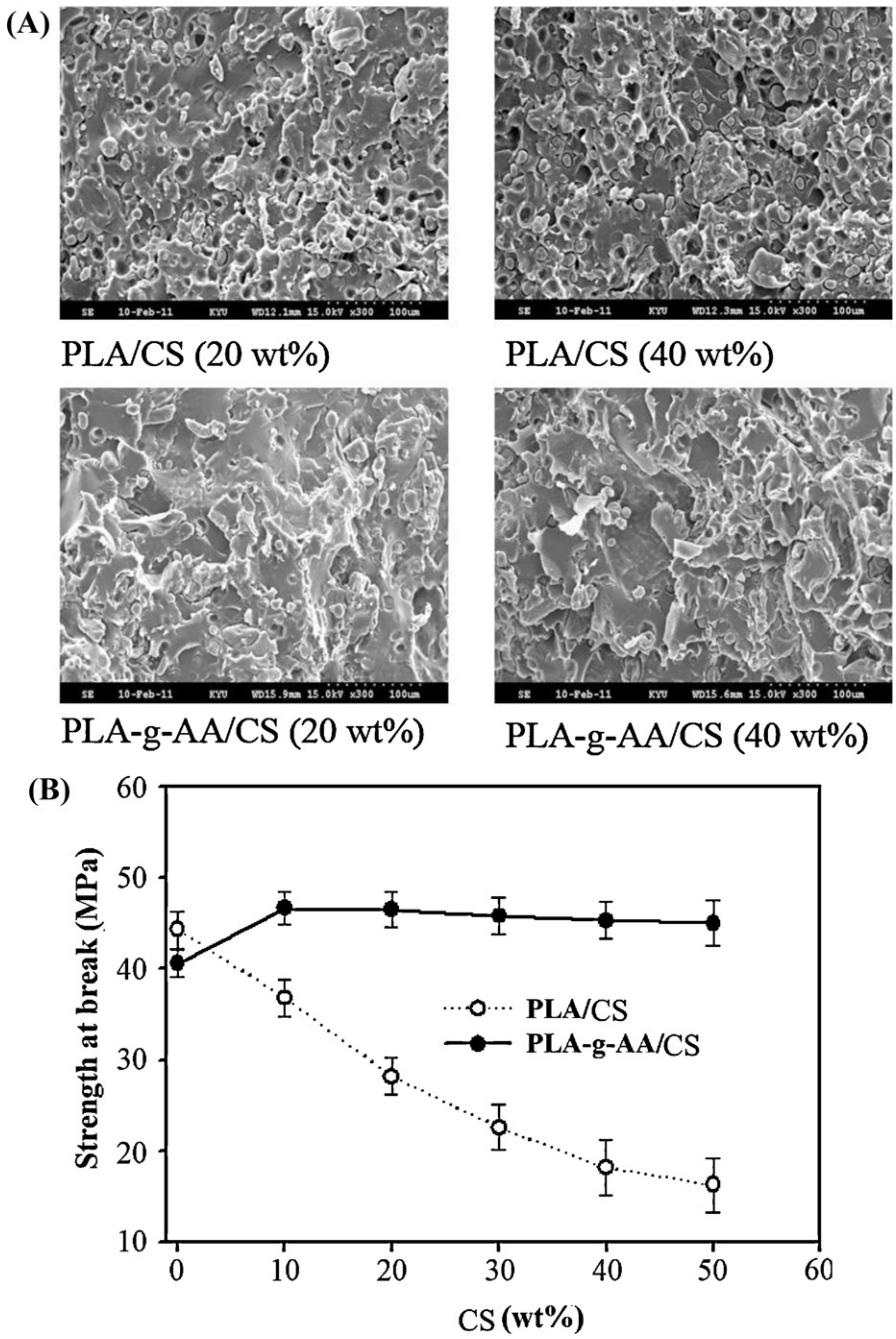

Fig. 4. (A) SEM micrographs of PLA/CS (20 wt%), PLA/CS (40 wt%), PLA-g-AA/CS (20 wt%), and PLA-g-AA/CS (40 wt%) for the tensile strength at breakpoint (300× magnification). (B) Tensile strength at breakpoint versus CS content for PLA-g-AA/CS and PLA/CS composites.

mechanical incompatibility of the two polymers is significant. For PLA-g-AA/CS composites, though a decrease in tensile strength at breakpoint compared to the pure PLA was observed, this decrease was smaller than that of the equivalent uncompatibilized composites. The absolute value of tensile strength at breakpoint for all compatibilized composites was notably higher than that of their uncompatibilized counterparts. It was also evident that the PLA-g-AA/CS composites provided higher stable values of tensile strength when the CS content was above 10 wt%. The findings of Iovino, Zullo, Rao, Cassar, and Gianfreda (2008) regarding the mechanical properties of PLA-g-MA/starch composites are similar to those discussed in this study. It is evident that the mechanical properties strongly depend on the dispersion and phase size of CS in the PLA or PLA-g-AA matrix. With a smaller dispersed phase, an increase in mechanical properties, particularly the tensile strength, was observed.

3.3. Biodegradation and cell release of PLA and composite film bags by B. cepacia

The time-dependent changes in morphology of the PLA and PLA-g-AA/CS matrices that encapsulated *B. cepacia* cells were focused on the 20, 60, and 120 day periods (Fig. 5). At 20 days, cell growth occurred on the surface of the PLA matrix (Fig. 5B). Moreover, some erosion and cracking was evident on the matrix surface. At 60 days, disruption of the PLA matrix structure was more apparent (Fig. 5C). This degradation was confirmed by an increasing weight loss of the PLA matrix with incubation time (Fig. 6A) and reached nearly

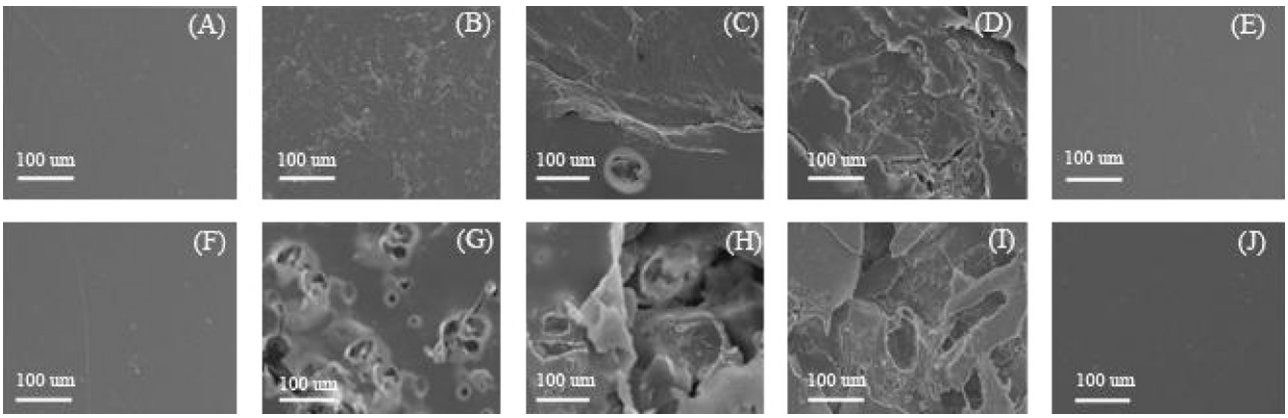

Fig. 5. Time-course SEM morphology of the PLA matrix loaded with *B. cepacia* cells (magnification of 300×): (A) 0 days, (B) 20 days, (C) 60 days, (D) 120 days, and (E) cell-free PLA matrix (120 days). Time-course morphology of the PLA-g-AA/CS (20 wt%) matrix with BEFB loaded with *B. cepacia* cells (300× magnification) (F) 0 days, (G) 20 days, (H) 60 days, (I) 120 days, and (J) cell-free PLA-g-AA matrix (120 days).

30% after 120 days. The most likely cause of this weight loss was biodegradation by *B. cepacia*, because the PLA is biodegradable. Reports in the literature have described the bacterial degradation of PLA (Abou-Zeid, Muller, & Deckwer, 2004; Cheung, Lau, Pow, Zhao, & Hui, 2010; Gattin, Copinet, Bertrand, & Couturier, 2002).

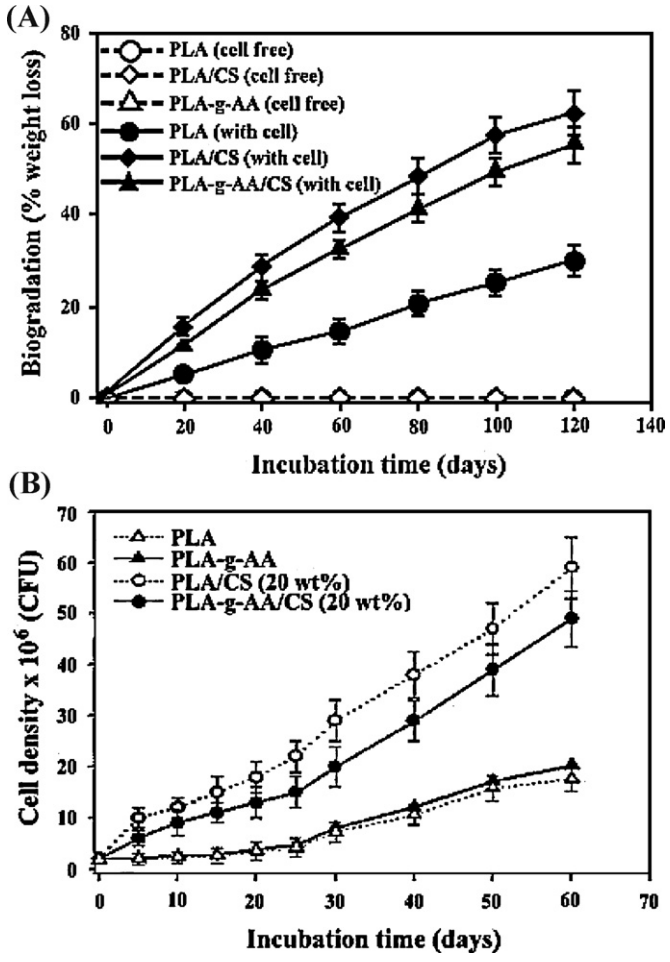

Fig. 6. (A) Time course for biodegradation (percent weight loss) of PLA, PLA-g-AA, and PLA-g-AA/CS (20 wt%) loaded with *B. cepacia* cells. (B) Time-course release and growth of *B. cepacia* cells entrapped in PLA, PLA-g-AA, PLA/CS (20 wt%), and the PLA-g-AA/CS (20 wt%) matrix suspended in saline solution.

These results show that *B. cepacia* is effective in degrading PLA. The PLA-g-AA/CS (20 wt% of CS) composite appeared to be degraded more readily by *B. cepacia*. At 20 days, a biofilm of bacterial cells was evident on the surface of the PLA-g-AA/CS (Fig. 5G), indicating more abundant cell growth than on PLA at 20 days. Moreover, larger pores were observed on the PLA-g-AA/CS composite at 60 and 120 days (panels H and I of Fig. 5), indicating a higher level of destruction. The weight loss of the PLA-g-AA/CS composite was also accelerated compared with that of the PLA and exceeded 55% after 120 days (Fig. 6A).

These results clearly indicate that the addition of CS enhanced the biodegradability of the composite, and may facilitate the release of entrapped cells into the environment. Thus, the release of BEFB can be controlled by the addition of biodegradable supplements, such as corn starch, into the core matrix, with higher levels of supplement leading to a more rapid release.

These results indicate the significant bacterial destruction of the matrix during the course of the incubation. Next, the time-course profile for cell release was examined. After a 120-day incubation, the final cell concentration in the saline solution was between 2.0×10^7 and 6.2×10^7 CFU/mL (Fig. 6B), indicating that the cells were released into the solution and remained viable. The cell-release pattern was similar for the PLA and PLA-g-AA/CS matrix, while the levels and rate of release differed. Fig. 6B shows that the rate of cell release was noticeably lower in the first 60 days than in the remaining incubation period, particularly for the PLA/CS and PLA-g-AA/CS composites. During this earlier period, the increase in cell concentration was most likely due to the release of cells from leaks in the matrix. Following release, the cells in the saline solution may have become inactive or lysed due to a lack of substrate, resulting in a decrease in viable cell concentration and CFUs. The noticeable increase in CFUs from 60 days onwards may represent not only an increase in cell release, but also an increase in substrate. According to the SEM micrographs (Fig. 5), the matrix structure was severely damaged after 60 days, leading to the release of cells, in addition to the residual CS and PLA fragments or PLA-g-AA matrix, into the solution. These fragments then may then have acted as a substrate to facilitate cell growth. Because CS is more readily biodegradable than PLA, and the solution containing the PLA/CS and PLA-g-AA/CS matrix reached a higher final cell concentration with a more rapid increase in cell concentration between days 60 and 120, the addition of CS clearly displayed a positive effect on the number of cells released. As a result, the rate and number of cells released can be adjusted by altering the composition of the matrix materials.

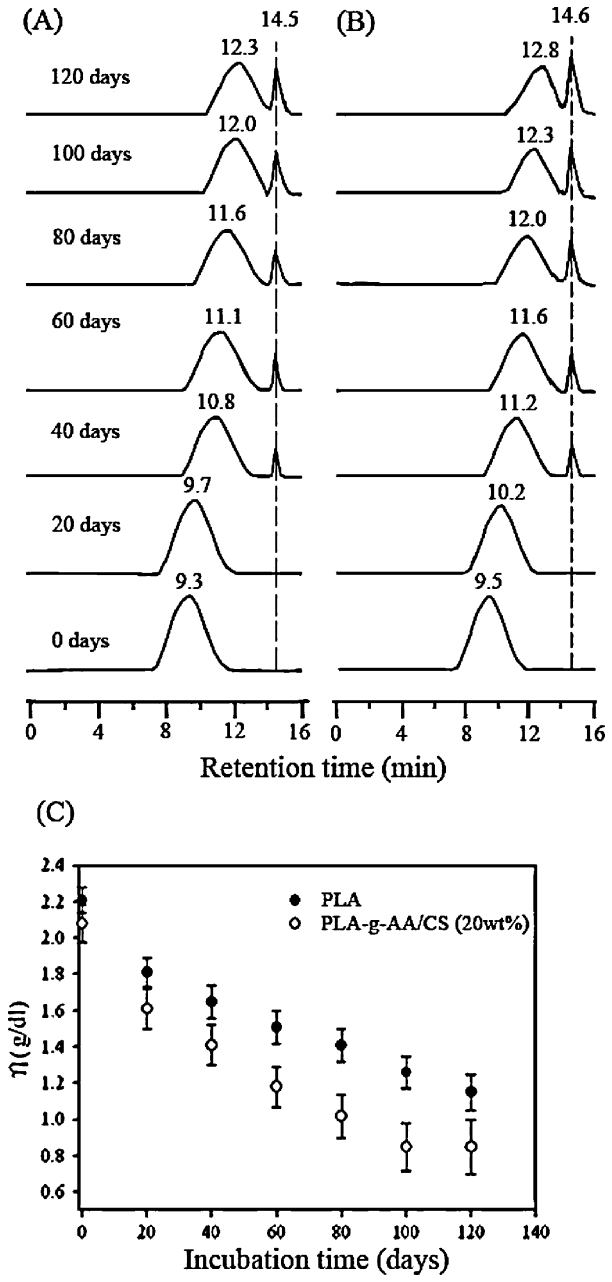

Fig. 7. (A and B) Time-course profiles of the retention time in the GPC analysis for PLA and PLA-g-AA/CS loaded with *B. cepacia* cells. (C) Time-course profile of the intrinsic viscosity for PLA and PLA-g-AA/CS loaded with *B. cepacia* cells.

3.4. Time-course measurement of GPC and intrinsic viscosity of PLA composites film bags by B. cepacia

The biodegradable PLA and PLA-g-AA/CS composite samples were analyzed using GPC, and the results are presented in Fig. 7A and B. The retention time of the major peaks (representing the original samples) increased with an increasing incubation time because the molecules within the original samples were continuously severed during the biodegradation process. The longer retention time of PLA-g-AA/CS also demonstrates its higher biodegradability than PLA. Additionally, a new peak appeared at ~14.5 to 14.6 min after 40 days of incubation, suggesting that some fragments were generated during the biodegradation of the PLA and PLA-g-AA/CS composites. The formation of fragments also indicates that CS had almost been depleted at this time. Zhao and Wilkins (2005) reported similar findings. The retention time of the fragments was approximately constant, which may have been due to the use of the depolymerized matrix as a substrate by the bacterium, producing nearly uniform fragments.

The change in intrinsic viscosity and molecular weight with incubation time for the PLA and PLA-g-AA/CS composites are demonstrated in Fig. 7C. The results show that the intrinsic viscosity for PLA encapsulating *B. cepacia* ranged from 2.21 to 1.16 g/dL over the 0–120 day incubation period, while the values for PLA-g-AA/CS were 2.08–0.85 g/dL. The lower intrinsic viscosity of the latter suggests that a higher number of fragments were present. Another cause of the decreased intrinsic viscosity of PLA-g-AA/CS is the conformational changes in the CS molecule caused by the formation of an ester functional group.

4. Conclusions

The compatibility and mechanical properties of CS blended with PLA and acrylic acid-modified PLA (PLA-g-AA) were examined. FTIR and Solid-state ^{13}C NMR analyses revealed the formation of ester groups from reactions between the —OH groups in CS and the carboxyl groups in PLA-g-AA, significantly altering the structure of the composite material. The morphology of the PLA/CS composites indicated that the CS phase size increased with increasing CS content, suggesting that compatibility between the PLA and CS was very poor. For PLA-g-AA/CS composites, the size of the CS phase was noticeably reduced and, being continually less than $9.0 \pm 1.0\,\mu m$, was detectable only under higher magnification. The tensile strength at breakpoint of the PLA/CS composites decreased markedly and continuously as the CS content increased. The composite containing PLA-g-AA exhibited enhanced mechanical properties compared with those containing PLA, particularly regarding the tensile strength at breakpoint. Finally, these results demonstrate that PLA-g-AA/CS (20 wt%) can be used to encapsulate cells of an indigenous phosphate-solubilizing bacterium (*B. cepacia* isolate) to form a controlled release bacterial fertilizer. The *B. cepacia* strain was able to degrade the BEFB materials, leading to cell release. The biodegradability of the BEFB depends on the type of material used, as a PLA capsule was also degraded, but to a lesser degree, and the addition of CS made the capsules more biodegradable. The decreases in intrinsic viscosity were also higher for the CS composite. Thereafter, the cell concentration in the saline solution increased significantly due to the release of cells from the severely damaged film bags, and cell growth by use of the depolymerized PLA-g-AA fragments as a substrate. The degree of biodegradation increased with increasing CS content. These results suggested that the release of fertilizer-promoted bacteria may be controllable via the formulation of a suitable film bag material.

References

Abou-Zeid, D.-M., Muller, R.-J., & Deckwer, W.-D. (2004). Biodegradation of aliphatic homopolyesters and aliphatic–aromatic copolyesters by anaerobic microorganisms. *Biomacromolecules*, *5*(5), 1687–1697.

Arvanitoyannis, I. S., Ladas, D., & Mavromatis, A. (2006). Potential uses and applications of treated wine waste: A review. *International Journal Food Science and Technology*, *41*(5), 475–487.

Cheung, H.-Y., Lau, K.-T., Pow, Y.-F., Zhao, Y.-Q., & Hui, D. (2010). Biodegradation of a silkworm silk/PLA composite. *Composites Part B: Engineering*, *41*(3), 223–228.

Cornelissen, T., Jans, M., Yperman, J., Reggers, G., Schreurs, S., & Carleer, R. (2008). Flash co-pyrolysis of biomass with polyhydroxybutyrate: Part 1. Influence on bio-oil yield, water content, heating value and the production of chemicals. *Fuel*, *87*(12), 2523–2532.

Dias, A. B., Müller, C. M. O., Larotonda, F. D. S., & Laurindo, J. B. (2010). Biodegradable films based on rice starch and rice flour. *Journal of Cereal Science*, *51*(2), 213–219.

Gattin, R., Copinet, A., Bertrand, C., & Couturier, Y. (2002). Biodegradation study of a starch and poly(lactic acid) co-extruded material in liquid, composting and inert mineral media. *International Biodeterioration and Biodegradation*, *50*(1), 25–31.

Gong, Q., Wang, L.-Q., & Tu, K. (2006). In situ polymerization of starch with lactic acid in aqueous solution and the microstructure characterization. *Carbohydrate Polymers*, *64*(4), 501–509.

Gupta, B., Revagade, N., & Hilborn, J. (2007). Poly(lactic acid) fiber: An overview. *Progress in Polymer Science*, *32*(4), 455–482.

Gupta, A. P., & Kumar, V. (2007). New emerging trends in synthetic biodegradable polymers–polylactide: A critique. *European Polymer Journal*, *43*(10), 4053–4074.

Hamdali, H., Hafidi, M., Virolle Marie, J., & Ouhdouch, Y. (2008). Growth promotion and protection against damping-off of wheat by two rock phosphate solubilizing actinomycetes in a P-deficient soil under greenhouse conditions. *Applied Soil Ecology*, *40*(3), 510–517.

Huang, C.-Y., Roan, M.-L., Kuo, M.-C., & Lu, W.-L. (2005). Effect of compatibiliser on the biodegradation and mechanical properties of high-content starch/low-density polyethylene blends. *Polymer Degradation and Stability*, *90*(1), 95–105.

Iovino, R., Zullo, R., Rao, M. A., Cassar, L., & Gianfreda, L. (2008). Biodegradation of poly(lactic acid)/starch/coir biocomposites under controlled composting conditions. *Polymer Degradation and Stability*, *93*(1), 147–157.

Jacobsen, S., Fritz, H.-G., Degee, P., Dubois, P., & Jerome, R. (2000). New developments on the ring opening polymerisation of polylactide. *Industrial Crops and Products*, *11*(2–3), 265–275.

Janorkar, A. V., Luo, N., & Hirt, D. E. (2004). Surface modification of an ethylene–acrylic acid copolymer film: Grafting amine-terminated linear and branched architectures. *Langmuir*, *20*(17), 7151–7158.

Junli, H., Xiangui, L., Junhua, W., Haiyan, C., Rui, Y., & Jiabao, Z. (2009). Population size and specific potential of P-mineralizing and solubilizing bacteria under long-term P-deficiency fertilization in a sandy loam soil. *Pedobiologia*, *53*(1), 49–58.

Kayserilioglu, B. S., Bakir, U., Yilmaz, L., & Akkas, N. (2006). Use of xylan, an agricultural by-product, in wheat gluten based biodegradable films: Mechanical, solubility and water vapor transfer rate properties. *Bioresource Technology*, *87*(3), 239–246.

Kidd, P. S., Domínguez-Rodríguez, M. J., Díez, J., & Monterroso, C. (2007). Bioavailability and plant accumulation of heavy metals and phosphorus in agricultural soils amended by long-term application of sewage sludge. *Chemosphere*, *66*(8), 1458–1467.

Kumar, H., Bajpai, V. K., Dubey, R. C., Maheshwari, D. K., & Kang, S. C. (2010). Wilt disease management and enhancement of growth and yield of *Cajanus cajan* (L.) var. Manak by bacterial combinations amended with chemical fertilizer. *Crop Protection*, *29*(6), 591–598.

Liu, B., Jiang, L., Liu, H., & Zhang, J. (2010). Synergetic effect of dual compatibilizers on in situ formed poly(lactic acid)/soy protein composites. *Industrial and Engineering Chemistry Research*, *49*(14), 6399–6406.

Liu, C. H., Wu, J. Y., & Chang, J. S. (2008). Diffusion characteristics and controlled release of bacterial fertilizers from modified calcium alginate capsules. *Bioresource Technology*, *99*(6), 1904–1910.

Lu, Z., Lu, M., He, F., & Yu, L. (2009). An economical approach for D-lactic acid production utilizing unpolished rice from aging paddy as major nutrient source. *Bioresource Technology*, *100*(6), 2026–2031.

Mamta, Rahi P., Pathania, V., Gulati, A., Singh, B., Bhanwra, R. K., & Tewari, R. (2010). Stimulatory effect of phosphate-solubilizing bacteria on plant growth, stevioside and rebaudioside-A contents of Stevia rebaudiana Bertoni. *Applied Soil Ecology*, *46*(2), 222–229.

Nair, L. S., & Laurencin, C. T. (2007). Biodegradable polymers as biomaterials. *Progress in Polymer Science*, *32*(8–9), 762–798.

Nampoothiri, K. M., Nair, N. R., & John, R. P. (2010). An overview of the recent developments in polylactide (PLA) research. *Bioresource Technology*, *101*(22), 8493–8501.

Nyambo, C., Mohanty, A. K., & Misra, M. (2010). Polylactide-based renewable green composites from agricultural residues and their hybrids. *Biomacromolecules*, *11*(6), 1654–1660.

Pilla, S., Gong, S., O'Neill, E., Yang, L., & Rowell, R. M. (2009). Polylactide-Recycled wood fiber composites. *Journal of Applied Polymer Science*, *111*(1), 37–47.

Shah, A. A., Hasan, F., Hameed, A., & Ahmed, S. (2008). Biological degradation of plastics: A comprehensive review. *Biotechnology Advances*, *26*(3), 246–265.

Son, H. J., Park, G. T., Cha, M. S., & Heo, M. S. (2006). Solubilization of insoluble inorganic phosphates by a novel salt- and pH-tolerant Pantoea agglomerans R-42 isolated from soybean rhizosphere. *Bioresource Technology*, *97*(2), 204–210.

Sullad, A. G., Manjeshwar, L. S., & Aminabhavi, T. M. (2010). Novel pH-sensitive hydrogels prepared from the blends of poly(vinyl alcohol) with acrylic acid-*graft*-Guar gum matrixes for isoniazid delivery. *Industrial and Engineering Chemistry Research*, *49*(16), 7323–7329.

Torbica, A., HadnaCev, M., & Dapcevi, T. (2010). Rheological, textural and sensory properties of gluten-free bread formulations based on rice and buckwheat flour. *Food Hydrocolloids*, *24*(6–7), 626–632.

Tuominen, J., Kylma, J., Kapanen, A., Venelampi, O., Itvaara, M., & Seppala, J. (2002). Biodegradation of lactic acid based polymers under controlled composting conditions and evaluation of the ecotoxicological impact. *Biomacromolecules*, *3*(3), 445–455.

Wang, G., & Lis, A. (2008). Thermal decomposition and kinetics of mixtures of polylactic acid and biomass during copyrolysis. *Chinese Journal of Chemical Engineering*, *16*(6), 929–933.

Wang, K.-H., Wu, T.-M., Shih, Y.-F., & Huang, C.-M. (2008). Water bamboo husk reinforced poly(lactic acid) green composites. *Polymer Engineering and Science*, *48*(9), 1833–1839.

Wu, C. S. (2009). Renewable resource-based composites of recycled natural fibers and maleated polylactide bioplastic: Characterization and biodegradability. *Polymer Degradation and Stability*, *94*(7), 1076–1084.

Wu, C. S. (2005). A new biodegradable blends prepared from polylactide and hyaluronic acid. *Polymer*, *46*(23), 10017–10026.

Yu, L., Dean, K., & Li, L. (2006). Polymer blends and composites from renewable resources. *Progress in Polymer Science*, *31*(6), 576–602.

Zell, M. T., Padden, B. E., Paterick, A. J., Hillmyer, M. A., Kean, R. T., Thakur, K. A. M., & Munson, E. J. (1998). Direct observation of stereodefect sites in semicrystalline poly(lactide) Using 13C solid-state NMR. *Journal of the American Chemistry Society*, *120*(48), 12672–12673.

Zhao, J., & Wilkins, R. M. (2005). Low molecular weight polylactic acid as a matrix for the delayed release of pesticides. *Journal of Agricultural and Food Chemistry*, *53*(10), 4076–4082.